INTRODUCTION

Parkinson's disease (PD) is a neurodegenerative disease characterized by a depletion of nigrostriatal dopaminergic cells in the basal ganglia in the brain (Helmich et al., 2010; Hacker et al., 2012). Consideration of nonmotor disabilities in PD including behavioral disturbances that arise during dopamine replacement treatment has recently been increased (Moskovitz et al., 1978; Aarsland et al., 1999; Frucht et al., 1999; Voon et al., 2007; Antonini & Cilia, 2009; Lee et al., 2010).

Compulsive reward-seeking behaviors and pathological repetition of the behaviors that occur in impulse control disorders (ICD) often appear in PD patients and have surged to clinical importance in relation to dopaminergic treatment (Molina et al., 2000; Driver-Dunckley et al., 2003; Dodd et al., 2005; Weintraub et al., 2006; Reiff & Jost, 2011). The underlying pathophysiological mechanisms of ICD in PD are not fully understood yet, however, considering that the neurodegenerative process in PD affects not only the nigrostriatal system, but also the mesolimbic and mesocortical dopaminergic pathways, most literature converge toward the hyperstimulation hypothesis (Voon et al., 2007; Antonini & Cilia, 2009; Ray & Strafella, 2010; Lee et al. 2014). According to the hypothesis, medication doses compensating for the dopamine-depleted dorsal striatum overstimulate relatively less affected ventral striatal regions, and it is speculated that the disturbed neural networks implicated in the modulation of reinforcement learning, reward-seeking behaviors, inhibitory control and impulse regulation are relevant to the development of ICD in PD (Antonini & Cilia, 2009; MacDonald & Monchin, 2011; Reiff & Jost, 2011; Bonnet et al., 2012; Lee et al., 2014).

Models of addiction address that repetitive exposure to rewarding stimuli enhances the saliency value of the rewarding stimuli, weakens the inhibitory control and leads to pathologically repetitive and impulsive behaviors without regard to any negative consequences (Ma et al., 2010; Baler & Volkow, 2006; Bechara, 2005). In PD displaying ICD, dysfunctions of brain areas that are involved in reward-based learning, motivation, impulse control and decision making processes, namely, the orbitofrontal cortex, amygdala, hippocampus, cingulate, insula and striatum, have been revealed in lines of research observations (van Eimeren et al., 2010; Cilia et al., 2011; Bonnet et al., 2012; Lee et al. 2014). Cilia et al. (2008) observed resting-state hyperactivity in orbitofrontal cortex, hippocampus, amygdala and ventral pallidum in a right hemisphere in PD patients with pathological gambling, and confirmed that the drug-induced behavioral disturbances are possibly associated with the dysfunction of mesocorticolimbic network. In addition, a $H_2{}^{15}O$ PET study showed a medication-induced disruption of activity in inhibitory networks during a card selection game in PD gamblers (van Eimeren, 2010). Relative deficits in inhibitory control may interact with dopamine agonists and predispose any vulnerable PD patients to develop ICD (Ray & Strafella, 2010). Thereafter, we aimed to further investigate the spatial reorganization of resting state functional connectivity of striatum in PD affected by appearance of ICD.

Recent studies proposed that dopaminergic circuits in the striatum actively participate in modulation of default mode network (DMN) deactivation under conditions of self-directed processing (Kelly et al., 2009; Tomasi et al., 2009; MacDonald & Monchi, 2011; Dang et al., 2012). It has been demonstrated that the functional connectivity of DMN is impaired in PD individuals, which predisposes the patients to an early cognitive decline. Previous findings revealed that patients with PD displayed a differential pattern of deactivation

in the posterior cingulate cortex and the precuneus of DMN in comparison with healthy controls (van Eimeren, 2009). The connectivity changes of DMN are also evident in substance addicts and patients with similar psychiatric disorders (Goldstein et al., 2008; Broyd et al., 2009; Sutherland 2012; Ma et al., 2011). Thus, it remains to be elucidated the DMN integrity departs from the DMN patterns in HC and PDC when drug-induced behavioral features are present.

Resting-state functional magnetic resonance imaging (rs-fMRI) offers a means to assess the functional network of the brain (Fox & Raichle, 2007; Helmich et al., 2010; Fox & Greicius, 2010; Zhang & Raichle, 2010). Temporal coupling between the low frequency fluctuations of blood oxygen level-dependent (BOLD) signals as the consequence of neuronal dynamics propagated through anatomically connected regions is thought to reflect the functional network of the brain (Friston et al., 1994; Biswal et al., 1995; Ghosh et al., 2008; He et al., 2008). Numerous studies on neurodegenerative diseases and psychiatric disorders have been widely conducted to examine the alterations of intrinsic fluctuations using rs-fMRI (Wang et al., 2007; Di Martino et al., 2008; Greicius, 2008; Ma et al., 2010).

To date, the reorganizations of resting state functional connectivity of dopaminergic striatal networks and DMN have not been extensively studied in PD affected by ICD. In this study, we examined spatial remapping of functional networks of striatum using seed-based correlation analysis of rs-fMRI as well as the functional connectivity changes of DMN in PD controls and PD with ICD in comparison to healthy controls.

SUBJECTS AND METHODS

Subjects

Nine healthy subjects (HC; M:F = 5:4, age = 56.0±7.0 yo), eight PD patients without ICD (PDC; M:F = 5:3, age = 58.5±8.5 yo) and ten PD patients with ICD (PDICD; M:F = 7:3, age = 54.9±6.7 yo) were participated in the study (Table 1). The PD patients were diagnosed according to the criteria of the UK PD Brain Bank Society, and had been using dopaminergic medications for longer than 5 years. The PDICD patients were identified by the appearance of medication-related impulse control disorders including compulsive gambling, shopping, binge eating and hypersexuality. They were also tested with the fulfillment of the fourth edition of the Diagnostic and Statistical Manual of Mental Disorders Text Revision criteria (DSM-IV-TR, American Psychiatric Association, 2000) and no prior history of ICD before the disease development. Nor the PDC group had prior history of ICD. Patients with cognitive impairments (mini-mental status examination (MMSE) score below 26), history of psychiatric illnesses, drug or alcohol dependence, any neurological disorders other than PD, and neurosurgical procedures were excluded from the subject selection. Any participants taking anti-psychotics, anti-depressants and other drugs that may affect dopamine and serotonin systems except for anti-parkinsonian medications were also excluded.

All subjects were examined at medication-on states using the Unified Parkinson's disease Rating Scale (UPDRS), the Mini-mental Status Examination (MMSE), the Geriatric Depression Scale 30 items (GDS) and Hoehn and Yahr (HY) stage (Table 1). The severity of ICD in PD with ICD was assessed using the modified version of Minnesota Impulsive Disorders

Interview (mMIDI) (Lee et al., 2009) (Table 1). Demographic and clinical features of patients such as age, gender, duration of PD and daily dosages of dopaminergic drugs were collected and total daily levodopa equivalent dose (total LED) and agonist daily levodopa equivalent dose (agonist LED) were calculated as described previously (Lee et al., 2009) (Table 1).

Table 1. Demographic and Clinical Features of Healthy Controls, PD Controls and PD with ICD

	HC	PDC	PDICD
Age (SD)	56.0 (7.0)	58.5 (8.5)	54.9 (6.7)
Male/Female	5/4	5/3	7/3
Age at PD onset (SD), y	-	49.3 (8.6)	44.9 (5.3)
Disease duration (SD), y	-	9.3 (3.0)	10.0 (8)
MMSE score (SD)	28.1 (1.1)	28.4 (1.9)	27.8 (1.3)
GDS score (SD)	4.9 (4.8)	8.9 (3.7)	15.2 (10.7)
UPDRS III (SD)	-	16.4 (7.3)	16.9 (12.5)
HY stage (SD)	-	2.2 (0.5)	2.4 (0.5)
mMIDI score (SD)	0	0	10.3 (4.9)
Total LED (SD), mg/day	-	859.6 (437.3)	905.6 (348.5)
Agonist LED (SD), mg/day	-	115.0 (105.1)	261.0 (178.0)

Values are means (standard deviations). NA indicates not applicable.

HC = healthy control; PDC = Parkinson's disease patients without impulse control disorders; PDICD = Parkinson's disease patients with impulse control disorders; PD = Parkinson's disease; MMSE = minimental status examination; GDS = geriatric depression scale; UPDRS = unified Parkinson's disease rating scale; HY = Hoehn and Yahr; mMIDI = modified Minnesota impulse disorders interview; LED = levodopa equivalent dose

Image acquisition and preprocessing

Subjects underwent rs-fMRI scanning on a Siemens TRIO 3T MRI scanner (repetition time = 3500 ms, echo time = 30 ms, axial slices = 35, an image matrix = 256×256, pixel size = 0.9375×0.9375 mm^2, a slice thickness = 3.5 mm, interslice gap = 4.2 mm, 128 images), and were asked to lie motionless

and awake with their eyes closed. High resolution T1-weighted images in corresponding subjects for spatial normalization of the functional echo planar images (EPI) were also collected (repetition time = 1600 ms; echo time = 1.91 ms; matrix = 256×256, a pixel size = 0.9375×0.9375 mm^2, and thickness = 1 mm).

All functional images were preprocessed using SPM8 (Statistical Parametric Mapping, www.fil.ion. ucl.ac.uk/spm) implemented on MATLAB (2009b, http://www.mathworks.com). First of all, slice timing differences for all fMRI time series were corrected using the middle slice as a reference, and the first five images for each subject were discarded to ensure magnetization equilibrium. The rest of the functional EPI data were spatially realigned to the first slice using a least squares approach and a six parameter rigid body spatial transformation. Transformation parameters from coregistration of high–resolution T1 images for each subject to standard T1 template were acquired and applied to spatially normalize the resliced EPI data, resampled at a voxel size of 3 mm, and smoothed with an isotropic 8-mm FWHM Gaussian kernel. The data were screened to ensure that the head movement throughout the resting state scanning was less than 2 mm in any dimension.

Calculation of functional connectivity

The head of caudate nucleus, anterior putamen, posterior putamen and posterior cingulate cortex were defined by using population-based MRI statistical probabilistic anatomy maps (Lee et al., 2005). The fMRI time series extracted from the regions were used and averaged over left and right hemispheres to calculate the mean time course of each seed region. The

resultant four time courses representing three striatal seed regions and one posterior cingulate cortex (PCC) seed region were used to subsequently generate functional correlation maps.

The following steps were performed using REST for seed-based correlation analysis (Resting-state fMRI Data Analysis Toolkit v1.8, by Song Xiaowei, http://resting-fmri.sourceforge.net). First, the smoothed EPI data were low-pass filtered with a cutoff frequency of 0.01 - 0.08 Hz, and linear trends were removed for all data. For each participant, a voxel-wise correlation coefficient map was calculated for each seed region-of-interest (ROI) by multiple regressions using averaged time courses of all the voxels in the seed ROI as a regressor, and a set of six motion correction parameters and whole brain, cerebrospinal fluid and white matter signals as nuisance variables. The resultant t-score maps were transformed by Fisher's z transform for further analysis as functional connectivity maps.

Statistical analysis

For group-level analysis, repeated measures ANCOVA was carried out with factors GROUP (HC, PDC and PDICD) and REGION (caudate head, anterior putamen, posterior putamen, and PCC), and a nuisance variable of age using SPM8. The statistical group comparison was performed in HC versus PDC, HC versus PDICD, and PDC versus PDICD for functional connectivity maps of each seed region thresholded at uncorrected $p<0.005$ and cluster size of >10.

RESULTS

Functional connectivity in healthy conditions

Striatal seed regions yielded strictly positive correlations in subcortical areas and patterns of functional connectivity generally consistent with previous findings as illustrated in Fig. 1 (Di Martino et al., 2008; Helmich et al., 2010; Hacker et al., 2012). The caudate was strongly correlated with medial frontal and fronto-polar regions, superior temporal cortex, anterior cingulate and thalamus (Fig. 1a). The anterior putamen was functionally connected to the medial frontal gyrus, parahippocampal gyrus, anterior and posterior cingulate, inferior frontal gyrus, bilateral middle frontal gyrus, right inferior parietal lobule and thalamus (Fig. 1b). The posterior putamen showed strong correlations with the left cerebellum, parahippocampal gyrus, anterior cingulate, medial frontal gyrus, left postcentral gyrus and thalamus extending down to the pons of brainstem (Fig. 1c). The functional connectivity of posterior cingulate cortex was found in core regions associated with the brain's default network including medial prefrontal cortex, inferior parietal lobule and lateral temporal cortex in healthy subjects (Fig. 1d).

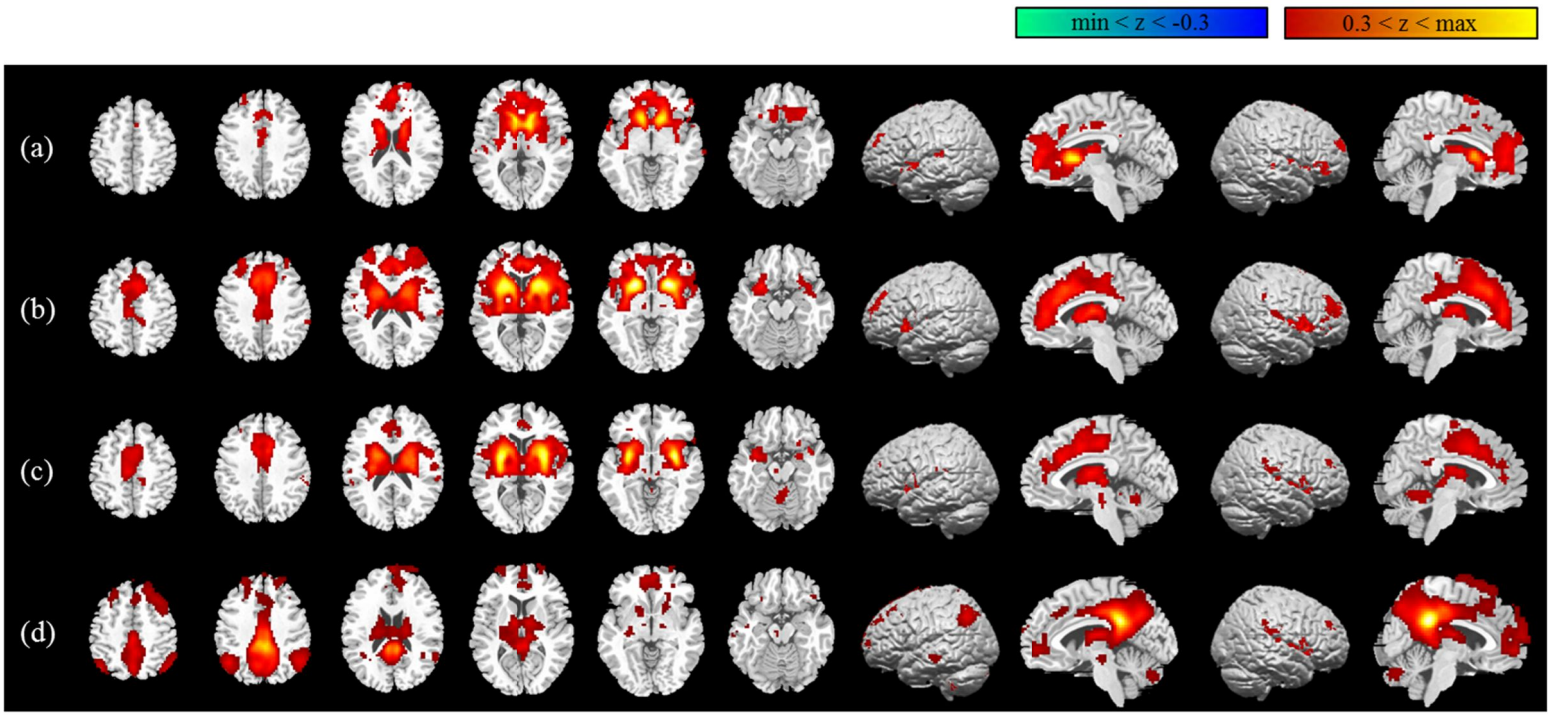

Figure 1. Functional connectivity of **(a)** head of caudate nucleus, **(b)** anterior putamen, **(c)** posterior putamen and **(d)** posterior cingulate cortex, averaged over subjects in HC group

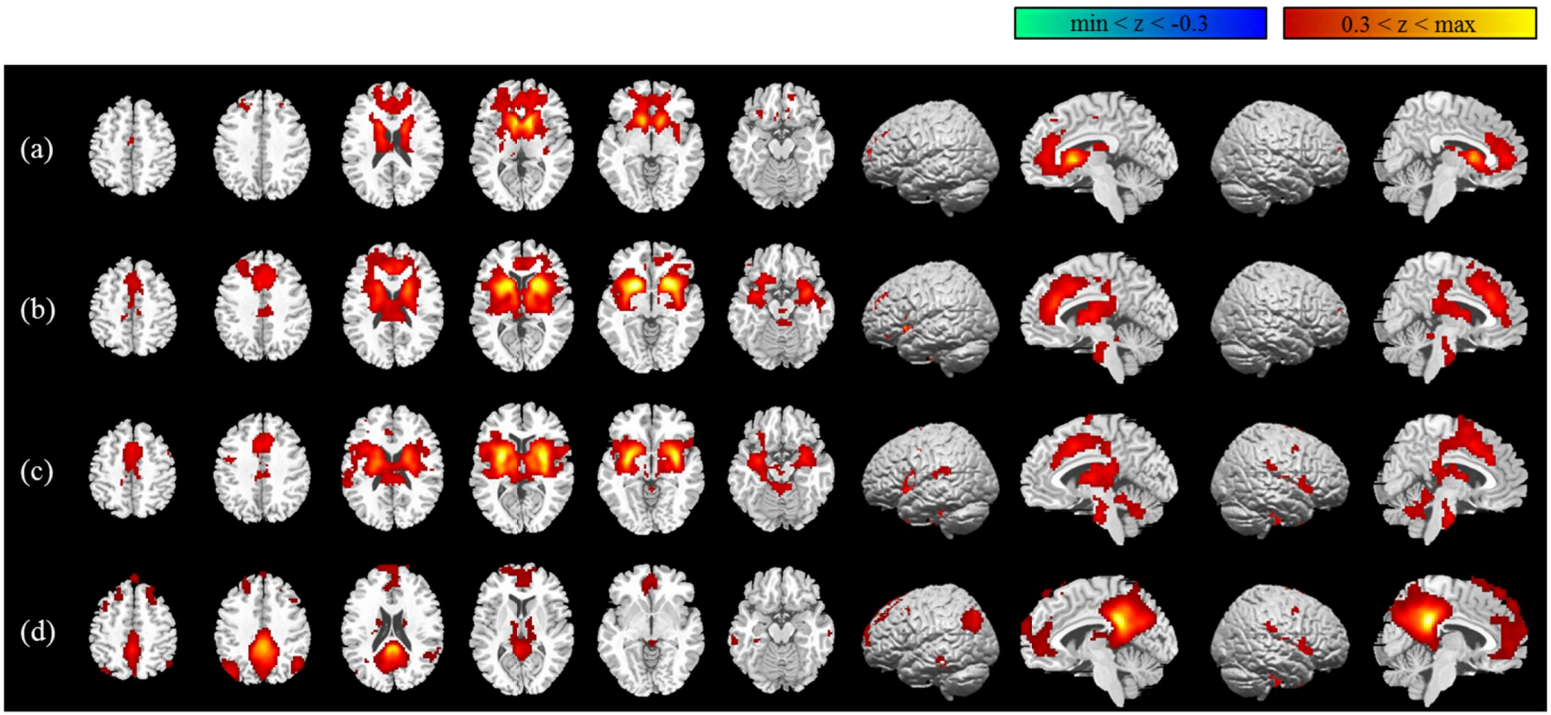

Figure 2. Functional connectivity of **(a)** head of caudate nucleus, **(b)** anterior putamen, **(c)** posterior putamen and **(d)** posterior cingulate cortex, averaged over subjects in PDC group

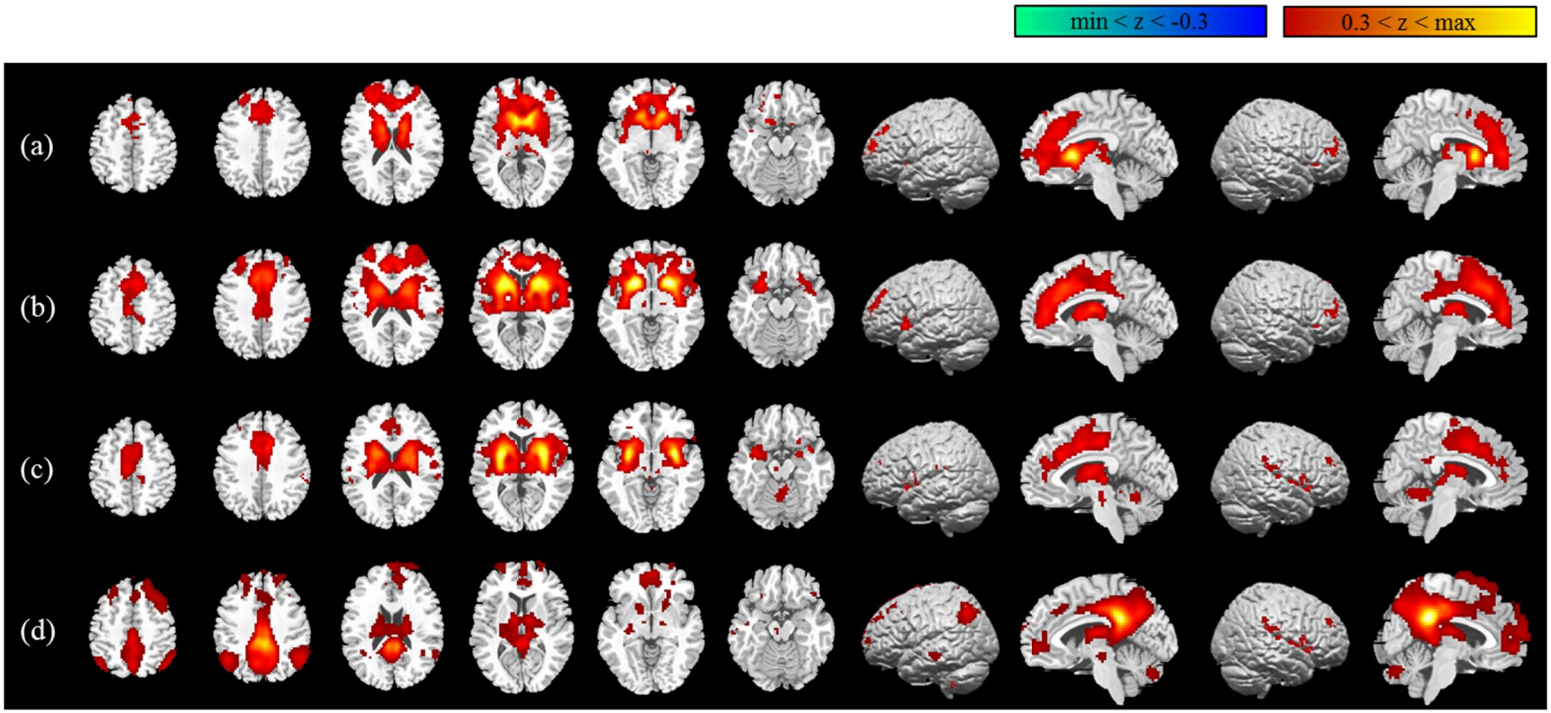

Figure 3. Functional connectivity of **(a)** head of caudate nucleus, **(b)** anterior putamen, **(c)** posterior putamen and **(d)** posterior cingulate cortex, averaged over subjects in PDICD group

Comparison of HC and PDC in striatal functional connectivity

As summarized in Table 2, the functional connectivity of the striatum was relatively weakened in many cortical regions in PDC compared to HC (Fig. 2). The head of caudate nucleus displayed a decreased functional connectivity in bilateral superior and middle frontal cortex (Brodmann area (BA) 10, 46), right inferior parietal lobule, bilateral inferior temporal gyrus (BA 20), right superior temporal gyrus (BA 23, 22), bilateral cingulate (BA 24), right orbitofrontal gyrus (BA 47), left precuneus (BA 7), right fusiform gyrus (BA 37, 20) and right superior parietal lobule (BA 7) (Fig. 4a). The PDC showed a weaker functional connectivity of the anterior putamen with the left superior temporal cortex (BA 22), right inferior parietal lobule (BA 40) and the left precentral gyrus (BA 6, 44) (Fig. 4b), while the posterior putamen was functionally dissociated in the right cingulate (BA 32) and bilateral cerebellum (Fig. 4c).

The functional enhancements with respect to striatal regions in PDC compared to HC were found commonly in the parahippocampal gyrus encompassing the hippocampus and amygdala (Table 2, Fig. 4). The increased functional connectivity in PDC was additionally found between the caudate head and the left superior frontal gyrus (BA 10), between the anterior putamen and the superior/middle temporal gyrus (BA 20, 38), and between the posterior putamen and medulla, cerebellum, left posterior cingulate and fusiform gyrus (BA 37) (Table 2).

Comparison of HC and PDICD in striatal functional connectivity

In PD patients displaying any form of ICD, the functional connectivity of the caudate head showed a similar pattern of impairments as seen in HC versus PDC (Table 3, Fig. 3, 5a). The regions that were found with reduced functional coupling with the caudate head were the bilateral cingulate gyrus (BA 24, 23, 31), right supramarginal gyrus, bilateral superior/middle temporal gyrus (BA 21, 39, 22, 20), inferior temporal gyrus (BA 20), superior frontal gyrus (BA 10), left orbitofrontal gyrus (BA 11), left precentral gyrus and cerebellum. PDICD displayed diminished functional correlations of the anterior putamen with the left precuneus (BA 7), right medial frontal gyrus (BA 10), cingulate cortex (24, 23, 31), right inferior parietal lobule (BA 40), left superior temporal gyrus (BA 22), thalamus and bilateral cerebellum compared to HC (Table 3, Fig. 5b). Reductions in the functional correlations with the posterior putamen were observable in the cingulate (BA 24), left precuneus (BA 7), right superior and inferior frontal cortex (BA 47), thalamus, right superior temporal gyrus (BA 39) and right cerebellum Table 3, Fig. 5c).

As illustrated in Fig. 5, the functional connectivity was stronger in PDICD between the caudate head and right parahippocampal gyrus (BA 30), midbrain, left superior frontal gyrus and lingual gyrus (Table 3, Fig. 5a). The enhanced functional correlations with the anterior putamen were also present in the bilateral parahippocampal gyrus, right insular cortex (BA 38), right superior temporal gyrus (BA 38) and thalamus, while the posterior putamen was functionally more correlated with the left parahippocampal gyrus and bilateral insula (BA 13) as seen in Fig. 5b, 5c and Table 3.

Comparison of PDC and PDICD in striatal functional connectivity

The functional connectivity of the caudate head did not show any significant impairments in PD individuals with ICD compared to those without it (Fig. 6a). Figure 6b and 6c display that the functional connectivity of the anterior putamen with the right cerebellum, thalamus, bilateral inferior temporal gyrus (BA 37, 20), orbitofrontal gyrus (BA 47) and cingulate (BA23) was more severely affected in PDICD, and the posterior putamen was functionally disconnected with the bilateral cerebellum, right superior frontal cortex (BA 10), left medial frontal and middle frontal cortex (BA 10, 6), left inferior temporal gyrus (BA 37), thalamus and cingulate (BA 23) (Table 4).

In Fig. 6, PDICD displayed a stronger functional connectivity of the caudate head with the bilateral middle frontal cortex (BA 10, 6), as well as with the left cerebellum and parahippocampal gyrus. The anterior putamen connectivity was enhanced PDICD in bilateral lingual gyrus (BA 18), right cuneus (BA 17), bilateral postcentral and precentral gyrus (BA 3, 4, 6, 34, 40), insula (BA 13), left inferior parietal lobule (BA 40) and occipital cortex (Table 4, Fig. 6b). The posterior putamen had functional enhancements only in the anterior cingulate (BA 24) in PDICD compared to PDC (Fig. 6c).

Functional connectivity changes of DMN

PDC in comparison to HC displayed functional connectivity reductions of PCC in the bilateral inferior parietal lobule (BA 40), cingulate (BA 24) and left precuneus (BA 7) within DMN and also in the left inferior frontal gyrus and cerebellum, although the right cuneus of DMN and right middle temporal

gyrus outside DMN showed relatively heightened functional connections (Table 2, Fig. 4d). PDICD had severely impaired functional connectivity in the cingulate cortex within DMN as well as in the inferior and middle frontal cortex (BA 6, 8, 47) and thalamus outside DMN in comparison to HC, despite relative increases within the posterior cingulate cortex itself and in parahippocampal gyrus (Table 3, Fig. 5d). The reductions in the functional connectivity of PCC in PDICD in comparison to PDC in Fig. 6d were found in the right inferior temporal cortex (BA 37), left fusiform gyrus (BA 20), as well as in the bilateral middle frontal cortex (BA 6, 21) and medial frontal cortex (BA 10). The DMN functional connectivity in PDICD versus PDC was enhanced in the right inferior parietal lobule (BA 24, 40), cingulate (BA 24, 31), middle and inferior frontal cortex (BA 46) and bilateral lingual gyrus (BA 18) (Table 4, Fig. 6d).

Table 2. Comparisons of striatal and DMN connectivity between HC and PDC

Contrast	Region	BA	Hemisphere	MNI coordinate			z-score
				x	y	z	
HC > PDC: Caudate head							
	Middle frontal gyrus	10	R	48	51	-3	3.80
		10	R	42	60	-3	2.80
		46	R	48	48	12	3.43
		6	L	-27	-12	45	3.24
	Inferior parietal lobule		R	48	-42	30	3.72
			R	48	-54	33	3.47
			R	42	-51	27	3.44
	Superior frontal gyrus	10	L	-15	66	21	3.65
		10	L	-9	60	27	2.86
	Inferior temporal gyrus	20	L	-57	-48	-18	3.55
		20	R	51	-9	-39	2.90
		20	R	45	-15	-42	2.88
	Uncus	20	R	30	-18	-38	3.50
	Cingulate	24	R	21	-3	45	3.47
		24	L	0	-12	30	3.42
	Superior temporal gyrus	23	R	57	9	-6	3.46
		22	R	54	-39	6	3.46
	Orbital gyrus	47	R	18	24	-27	3.32
	Precuneus	7	L	-18	-81	48	2.96
	Fusiform gyrus	37	R	45	-57	-18	2.96
		20	R	57	-12	-33	2.86
	Superior parietal lobule	7	R	21	-72	57	2.82
HC < PDC: Caudate head							
	Parahippocampal gyrus	30	R	12	-36	-6	3.21
	Superior frontal gyrus	10	L	-27	57	-3	3.08
HC > PDC: Anterior putamen							
	Superior temporal gyrus	22	L	-54	-12	6	3.40
	Inferior parietal lobule		R	48	-45	30	3.32
		40	R	48	-54	36	2.79
		40	R	42	-60	48	3.27
	Middle occipital gyrus	19	L	-36	-93	12	3.23
	Precentral gyrus	6	L	-30	-15	51	3.15
		44	L	-48	12	6	2.94
		44	L	-42	15	15	2.88
HC < PDC: Anterior putamen							
	Parahippocampal gyrus		R	33	-15	-24	4.29
			L	-30	-9	-18	4.19
	Superior/Middle temporal gyrus	20	L	-33	3	-48	3.64
		38	R	33	12	-45	2.87
HC > PDC: Posterior putamen							
	Cingulate	32	R	15	24	24	3.44
	Cerebellum		L	-6	-63	-6	3.31
			R	3	-66	-9	2.85
HC < PDC: Posterior putamen							

	Parahippocampal gyrus		L	-36	-9	-21	4.12
		35	R	27	-21	-21	3.38
			R	36	-18	-24	3.09
		28	L	-24	-18	-24	3.53
		28	L	-15	-15	-24	3.04
	Medulla			3	-21	-45	3.72
	Cerebellum		R	18	-33	-51	3.03
	Posterior cingulate	23	L	0	-33	21	2.90
	Fusiform gyrus	37	R	48	-57	-27	3.13
HC > PDC: Posterior cingulate cortex							
	Inferior parietal lobule	40	R	45	-57	39	3.87
			R	51	-42	33	2.79
		40	L	-60	-45	45	3.05
		40	L	-51	-57	51	2.64
	Cingulate	24	L	-3	-9	36	3.76
		24	R	3	-3	36	3.44
	Precuneus	7	L	-15	-72	42	3.62
		7	L	-18	-60	42	2.93
	Inferior frontal gyrus	11	L	-21	24	-9	3.35
	Cerebellum		R	30	-75	-33	3.35
HC < PDC: Posterior cingulate cortex							
	Middle temporal gyrus	39	R	48	-81	24	3.31
		21	R	66	-54	-3	2.73
		37	R	57	-57	-3	2.72
	Cuneus	18	R	12	-72	18	3.20

Table 3. Comparisons of striatal and DMN connectivity between HC and PDICD

Contrast	Region	BA	Hemisphere	MNI coordinate			z-score
				x	y	z	
HC > PDICD: Caudate head							
	Cingulate	24	L	0	-6	30	3.99
		23	L	0	-21	27	2.97
		31	R	15	-42	30	3.21
	Supramarginal gyrus		R	45	-54	27	3.46
	Superior/middle temporal gyrus	21	R	51	-42	6	3.34
		39	R	45	-54	15	3.20
		22	L	-66	-30	0	3.42
		20	R	54	-51	-15	3.03
	Inferior temporal gyrus	20	L	-57	-48	-18	3.40
		20	L	-57	-39	-27	3.12
		20	R	54	-12	-45	3.11
		20	R	45	-15	-42	2.72
	Superior frontal gyrus	10	L	-12	63	24	3.18
	Uncus	20	R	30	-18	-39	3.13
	Orbital gyrus	11	L	-9	24	-27	3.11
	Postcentral gyrus		L	-69	-24	36	3.06
	Cerebellum		L	-27	-90	-39	2.90
HC < PDICD: Caudate head							
	Parahippocampal gyrus	30	R	15	-33	-9	4.10
	Midbrain			9	-33	-18	3.21
	Superior frontal gyrus	10	L	-27	57	-6	3.13
	Lingual gyrus		L	-18	-84	-6	2.90
HC > PDICD: Anterior putamen							
	Precuneus	7	L	-12	-72	42	3.51
	Medial frontal gyrus	10	R	15	51	-3	3.39
	Cingulate	24	R	6	-3	36	3.35
		24	L	-9	-6	36	3.18
		24	R	6	6	30	2.73
		23	R	3	-27	-3	3.28
		31	L	0	-36	27	2.98
	Inferior parietal lobule	40	R	48	-63	51	3.33
		40	R	48	-54	36	3.11
			R	42	-54	27	2.87
	Superior temporal gyrus		L	-72	-24	-3	3.28
		22	L	-54	-12	6	3.23
	Thalamus		R	6	-18	12	3.26
			L	-6	-15	12	3.03
	Cerebellum		R	0	-81	-27	3.15
			R	27	-90	-36	3.06
			L	-12	-87	-27	2.98
HC < PDICD: Anterior putamen							
	Parahippocampal gyrus		L	-27	-12	-21	4.17
			L	-33	0	-15	3.23
			R	30	-15	-24	3.43
			L	-9	0	-21	3.19
		19	L	-33	-48	-6	3.18

	Insula	38	R	36	0	-9	3.55
	Superior temporal gyrus	38	R	33	15	-36	3.25
	Thalamus		L	-18	-33	-3	3.00
HC > PDICD: Posterior putamen							
	Cingulate	24	L	-9	-6	36	4.67
		24	R	6	-3	36	3.49
	Precuneus	7	L	-15	-69	42	3.26
		7	L	-12	-78	45	2.74
	Superior frontal gyrus		R	15	51	-9	3.16
	Inferior frontal gyrus	47	R	54	33	0	3.12
		45	R	45	30	3	2.78
		45	R	54	39	6	2.75
	Thalamus		L	-18	-12	18	3.09
	Superior temporal gyrus	39	R	42	-57	21	3.03
	Cerebellum		R	18	-93	-39	2.89
			R	39	-84	-39	2.88
			R	30	-90	-39	2.84
HC < PDICD: Posterior putamen							
	Parahippocampal gyrus		L	-33	0	-15	4.78
			L	-27	-15	-24	2.68
	Insula	13	L	-39	-6	-3	2.98
		13	R	39	-12	-9	3.58
		13	L	-33	-15	24	3.29
HC > PDICD: Posterior cingulate cortex							
	Cingulate	24	R	3	-3	33	3.39
		33	L	-3	9	27	3.19
		23	L	-3	-21	30	3.03
	Inferior frontal gyrus	47	L	-21	27	-3	2.94
		47	R	18	15	-27	3.13
	Middle frontal gyrus	6	L	-45	0	60	3.03
		8	L	-33	15	51	2.85
		8	L	-27	21	51	2.65
	Thalamus		L	-18	-24	15	2.94
HC < PDICD: Posterior cingulate cortex							
	Cingulate	31	L	0	-36	42	3.31
	Parahippocampal gyrus	35	L	-21	-21	-21	3.31
	Insula	13	L	-45	-12	15	3.01
	Lingual gyrus	18	L	-15	-81	-12	2.83

Table 4. Comparisons of striatal and DMN connectivity between PDC and PDICD

Contrast	Region	BA	Hemisphere	MNI coordinate			z-score
				x	y	z	
PDC > PDICD: Caudate head							
	None						
PDC < PDICD: Caudate head							
	Cerebellum		L	-9	-69	-9	3.21
	Middle frontal gyrus	10	L	-45	48	12	3.07
		6	R	24	-3	45	2.90
	Parahippocampal gyrus	27	L	-24	-30	-6	2.95
PDC > PDICD: Anterior putamen							
	Cerebellum		R	54	-60	-27	4.02
			R	15	-69	-48	3.59
			R	27	-69	-42	3.24
	Inferior temporal gyrus	37	R	60	-60	-18	2.77
		20	L	-48	-27	-24	3.18
	Orbital gyrus	47	R	21	18	-15	3.15
	Cingulate	23	L	-3	-33	24	3.80
	Thalamus		L	-9	-12	0	3.34
			L	-18	-9	12	2.97
PDC < PDICD: Anterior putamen							
	Lingual gyrus	18	R	15	-87	-9	3.32
		18	R	21	-75	-6	3.11
		18	L	-18	-81	-6	3.14
		18	L	-12	-66	-3	2.81
	Cuneus	17	R	18	-78	3	2.74
	Postcentral gyrus		L	-42	-21	30	3.28
		43	L	-54	-9	18	3.15
		40	R	39	-39	57	3.11
		3	R	45	-27	54	2.83
		3	L	-27	-36	57	2.75
		3	L	-36	-36	48	2.75
	Precentral gyrus	4	L	-33	-21	42	3.24
		6	L	-30	-15	51	3.17
		4	R	36	-21	39	3.19
		6	R	33	-15	48	2.96
		4	L	-57	-15	30	2.80
	Insula	13	L	-33	-15	24	3.12
			L	-36	-6	6	3.23
		13	R	33	-18	12	3.00
	Inferior occipital gyrus		R	39	-69	-9	2.95
	Inferior parietal lobule	40	L	-39	-42	57	2.95
PDC > PDICD: Posterior putamen							
	Cerebellum		L	-21	-69	-45	4.01
			R	51	-72	-39	3.75
			R	54	-60	-42	3.07
			R	12	-69	-48	3.43
			R	3	-69	-30	3.40
			R	18	-93	-39	3.29
			R	12	-84	-42	3.09

			R	33	-57	-36	3.28
			R	24	-57	-33	2.90
			R	54	-60	-27	3.28
	Superior frontal gyrus	10	R	12	69	21	3.54
		10	R	6	66	30	2.79
			R	18	54	-9	3.17
	Medial frontal gyrus	10	L	0	66	21	3.11
	Middle frontal gyrus	6	L	-45	6	51	3.31
	Inferior temporal gyrus	37	R	60	-60	-15	2.85
	Thalamus		L	-18	-15	9	3.04
			R	15	-15	6	3.03
	Cingulate	23	L	-9	-33	27	2.79
PDC < PDICD: Posterior putamen							
	Cingulate	24	L	-3	27	0	3.14
PDC > PDICD: Posterior cingulate cortex							
	Inferior temporal gyrus	37	R	63	-54	-9	3.49
	Fusiform gyrus	20	L	-51	-33	-27	3.27
	Middle frontal gyrus	21	L	-45	9	-33	3.12
		6	R	36	-6	66	3.12
		6	R	30	3	63	2.66
	Medial frontal gyrus	10	R	6	63	24	2.86
PDC < PDICD: Posterior cingulate cortex							
	Inferior parietal lobule	40	R	54	-48	39	3.69
		40	R	45	-54	39	3.51
		40	R	48	-51	27	2.94
	Cingulate	24	R	3	-21	39	3.45
		31	L	0	-36	45	3.42
		31	R	9	-36	39	3.37
	Middle frontal gyrus	46	R	54	24	30	3.31
	Inferior frontal gyrus	46	L	-48	48	6	3.26
	Lingual gyrus	18	R	3	-90	-15	3.11
		18	L	-12	-81	-15	3.04

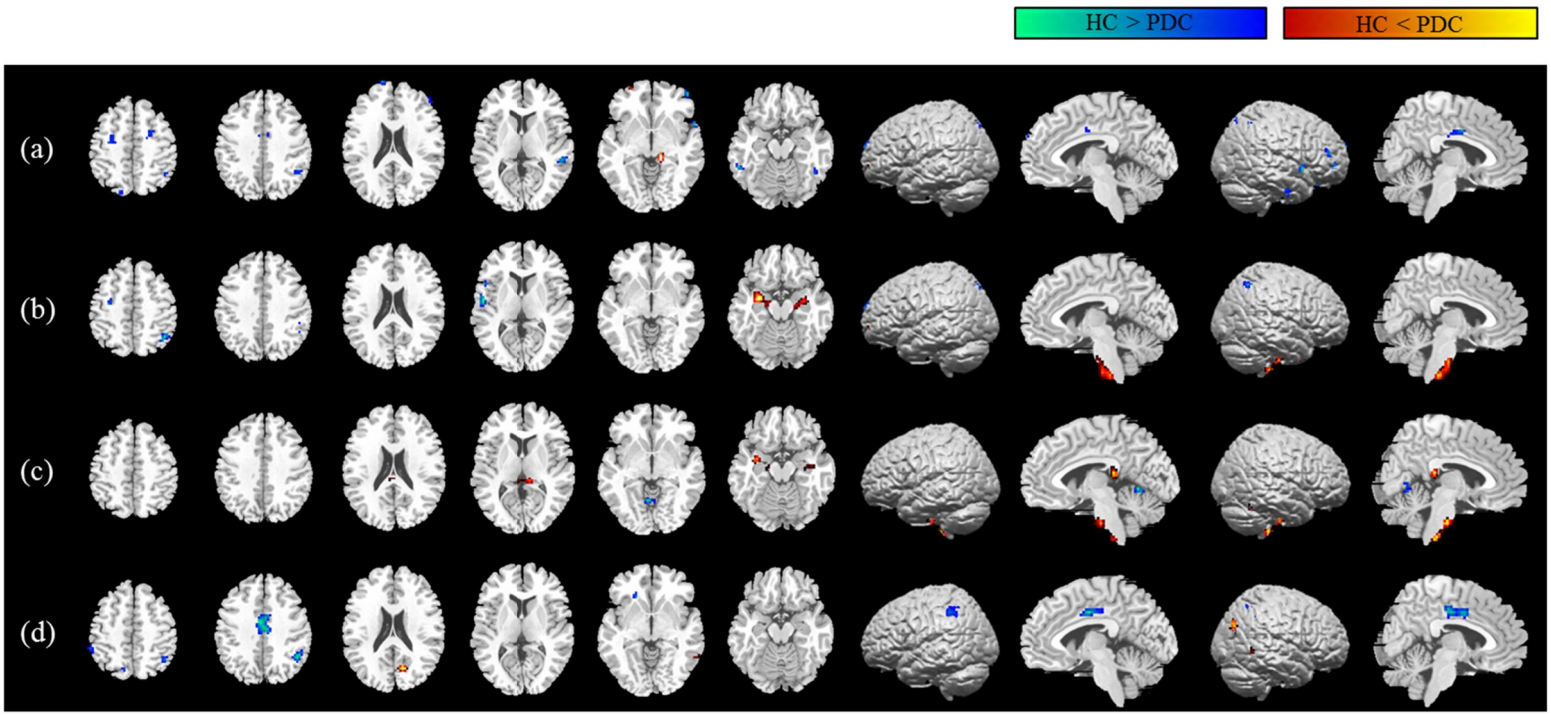

Figure 4. Functional connectivity changes of **(a)** head of caudate nucleus, **(b)** anterior putamen, **(c)** posterior putamen and **(d)** posterior cingulate cortex, in PDC compared to HC

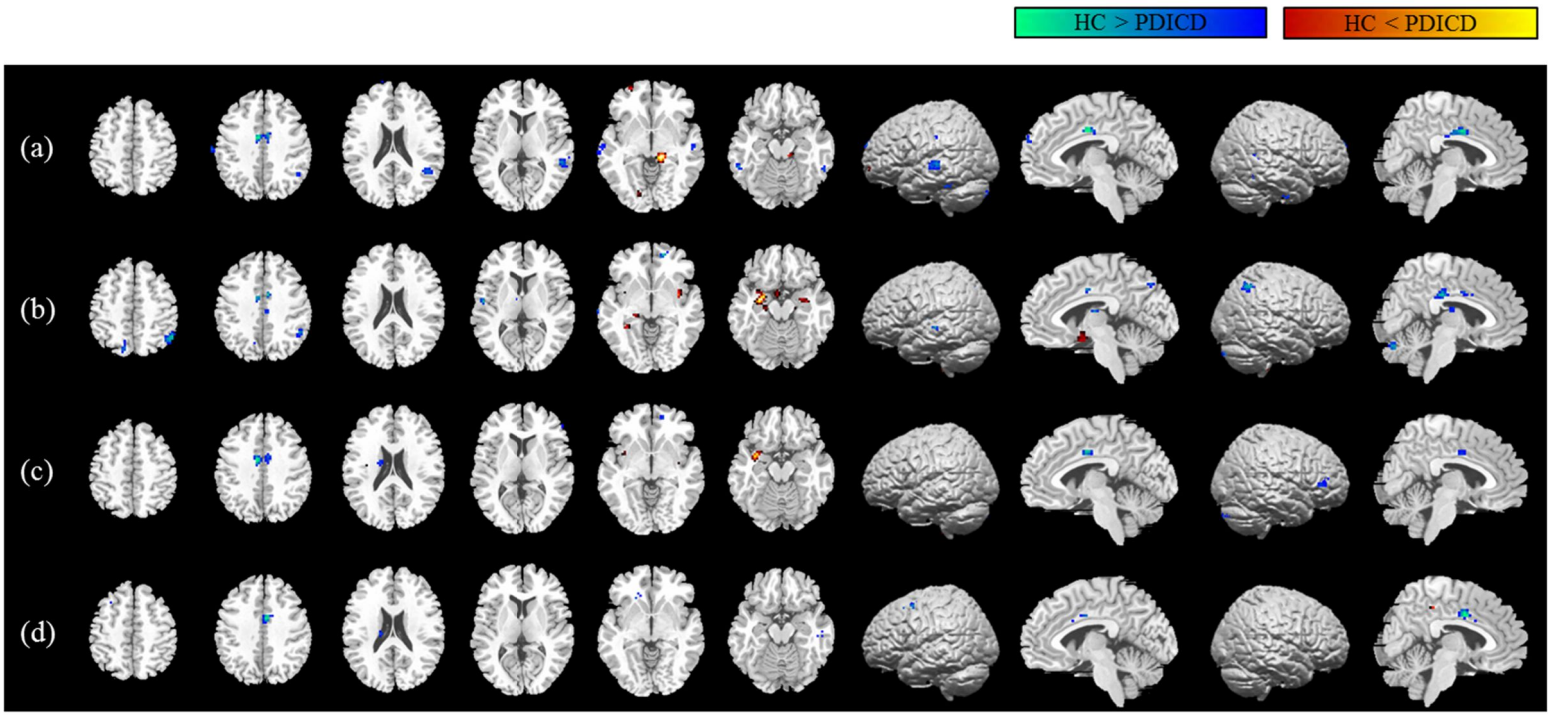

Figure 5. Functional connectivity changes of **(a)** head of caudate nucleus, **(b)** anterior putamen, **(c)** posterior putamen and **(d)** posterior cingulate cortex, in PDICD compared to HC

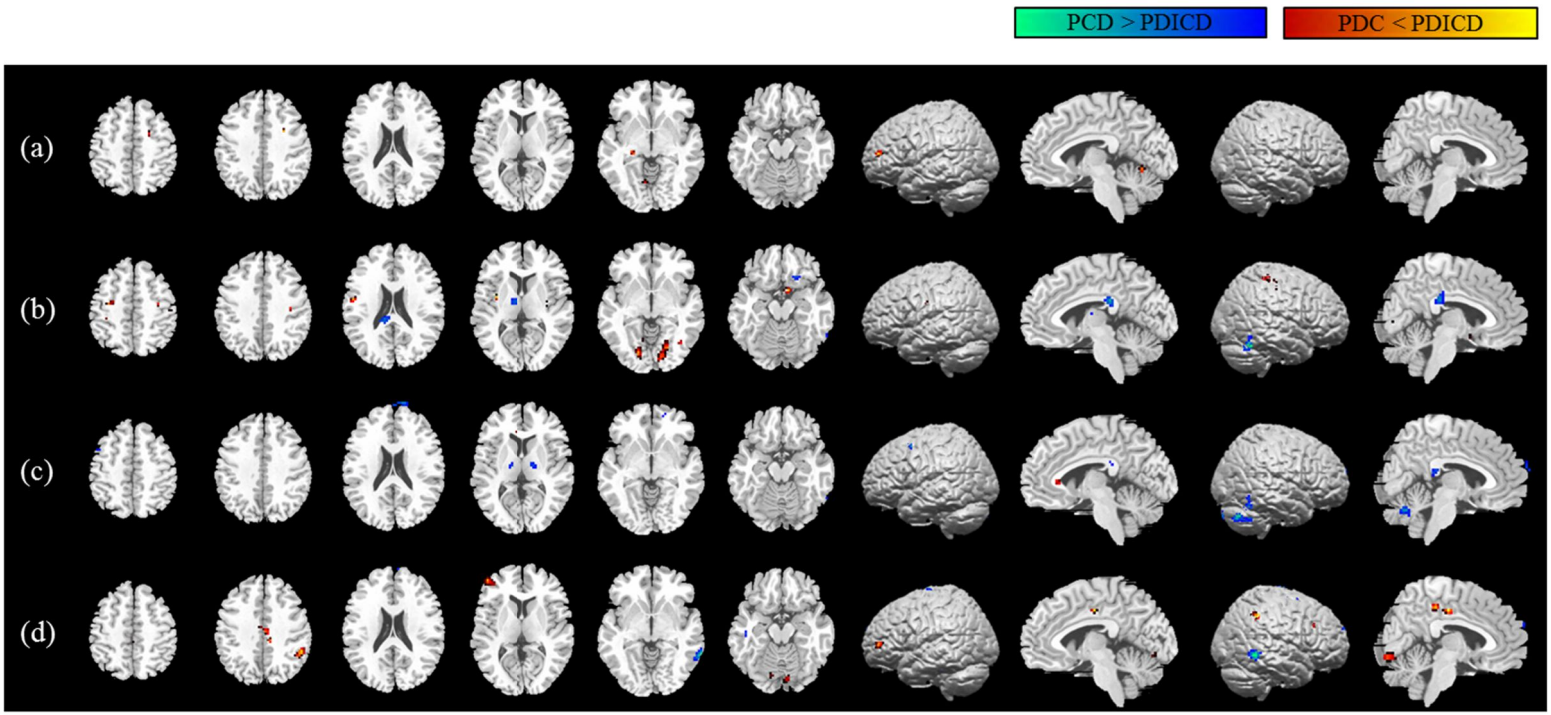

Figure 6. Functional connectivity changes of **(a)** head of caudate nucleus, **(b)** anterior putamen, **(c)** posterior putamen and **(d)** posterior cingulate cortex, in PDICD compared to PDC

DISCUSSION

The patterns of inter-regional functional couplings of striatum in our study followed the previous reports, where the caudate nucleus is strongly correlated with the regions that are implicated in emotional processing and executive function (Di Martino et al., 2008; Helmich et al., 2010; Hacker et al., 2012). The functional connectivity pattern of putamen mainly predicts the activity of cortical and subcortical motor areas, and the anterior portion of putamen exhibits a spatial pattern of positive functional correlations that lie intermediate between the head of caudate nucleus and posterior putamen, as has been evident in a previous study (Hacker et al., 2012). In diseased conditions as in Fig. 2 and 3, we observed that cortical functional connectivity of the striatum was, in overall, weakened in individuals with PD compared to those without the disease, as an outcome of degeneration of dopaminergic basal ganglia system, which is consistent with other previous findings (Helmich et al., 2010; Hacker et al., 2012). The functional connectivity of the caudate head in the striatum was substantially reduced in several cortical areas including cingulate, supramarginal gyrus, superior and middle frontal cortices and middle and inferior temporal cortices in both PDC and PDICD when compared to HC. The caudate receives projections mainly from prefrontal cortical areas, orbitofrontal cortex, cingulate and parahippocampal gyrus (Di Martino et al., 2008; Helmich et al., 2010; Hacker et al., 2012). In PD pathological condition, the weakening of the functional connectivity of the caudate with the medial prefrontal cortex in our study is consistent with the findings of a connectivity analysis (van Eimeren et al., 2009). It is also confirmed that the dopaminergic degeneration in PD substantially impairs not only the striatum, but also the prefrontal areas sufficiently to cause functional

impairments as the disease progresses (Owen et al., 1993; Rogers et al., 1998; Rakshi et al., 1999; Dagher et al., 2001). The functional weakening in the cortical areas in our study appears as PD-related pathological changes despite no cognitive deficits reported in the subjects.

The enhanced functional connectivity in parahippocampal gyrus and in the frontal lobe evident in both PD groups might be a case of compensatory phenomenon as a consequence of striatal dopamine depletion, or a case of plastic changes following overstimulation of relatively spared mesolimbic networks with dopaminergic medication. In PET activation study, mildly affected PD group performed as well as healthy controls in cognitive frontostriatal tasks, but displayed different activation patterns in caudate and hippocampus (Dagher et al., 2001). Hippocampal recruitment was accounted for by a compensatory mechanism to overcome striatal deficits in PD group, however, the contribution of medication effects was not considered.

PDC and PDICD groups in our study did not differ significantly in the patterns of the impaired functional organizations of the caudate head. We observed that the areas with reduced functional connectivity with the anterior putamen overlapped in the superior temporal gyrus and inferior parietal lobule in PDC and PDICD in comparison to healthy subjects. The patients without any ICD were more affected in supramarginal gyrus and left precentral gyrus, whereas PDICD suffered from severe functional impairments in the precuneus, medial frontal gyrus, cingulate, thalamus and cerebellum (Fig. 6b, c). This may imply that the addictive and repetitive behavioral changes in PD may be related to abnormal remapping of the putaminal connectivity induced by dopaminergic medications.

We observed that a heightened putaminal connectivity with the insular cortex was shown in PDICD, which was absent in PDC group (Fig. 6b). The

insular cortex is recently found to be related to addictive behaviors (Naqvi et al., 2007; Naqvi & Bechara, 2008), and its enhanced functional connection with the putamen in PDICD in our study may imply that greater insular connectivity is established as an outcome of repetitive and addictive behavior following the drug-induced overstimulation of limbic system. We can assume that functional hyperconnectivity between the putamen and insular cortex and between the caudate head and parahippocampal gyrus observed in PDICD reflects that a network involving these regions is affected by the psychiatric condition. Consistently, it has been reported that the networks implicated in impulse regulation that are thought to mediate inhibitory control during decision-making and response monitoring are functionally disrupted in drug addicts and pathological gamblers (van Eimeren 2010). The functional overactivity in a network involving the orbitofrontal cortex, hippocampus, amygdala, insula and ventral striatum has been found in PD patients with pathological gambling at resting state (Cilia et al., 2008). Additionally, the resting state activity of areas including the ventrolateral prefrontal cortex, cingulate, medial prefrontal cortex, insula, striatum and parahippocampal gyrus displayed a statistically significant correlation with the severity of pathological gambling behaviors in PD (Cilia et al., 2011). Our findings provide evidence that the functional alterations of the parahippocampal cortex and insula which are the areas crucial for impulse control and response inhibition, either result from the drug-induced behavioral changes or evoke behavioral disturbances in vulnerable individuals. The causal relationship of the functional alterations and appearance of ICD in PD need to be elucidated in future studies.

The cerebellar disconnections of the posterior putamen were observed in PD individuals, although they seemed more severe in PD associating ICD. The cerebellar dysfunction appears as disease-specific processes, and supports

the clinical relevance of cerebellar circuits to basal ganglia to parkinsonism as demonstrated in Hacker et al. (2012). The functional correlations with the anterior putamen are heightened in the postcentral and precentral cortices in PDICD relative to PDC group, and this may arise due as a compensatory change in functional connectivity for dopaminergic depletion in basal ganglia and cerebellum.

In our results, it was notable that the thalamic activity in the striatal network is dysfunctional in PDICD (Fig. 5b, c & 6b, c). The thalamus is well known as a relay station between subcortical structures and cortical areas in various neural pathways including motor-related system and reward processing and impulse control systems. It has been suggested that the thalamus integrates activity and relays information, modulating dopaminergic reward system (Rieck et al., 2004). In a previous study, presentation of gambling cues suppressed the activity of the thalamus, basal ganglia, and frontal and orbitofrontal cortex in pathological gamblers compared to healthy controls (Potenza et al., 2003). We can speculate that since the thalamic networks play a role in reward processing and inhibitory impulse control in addictive process, the dysfunction of the thalamus presents the vulnerable patients more prone to fail to convey negative feedbacks and continue to engage in repetitive and impulsive activities despite disastrous consequences brought by the behaviors.

The default mode network (DMN) comprises the brain areas that are actively synchronized in the attention and self-monitoring processes, and refers to the deactivation pattern during transition from resting state to cognitive demanding conditions (Ma et al., 2011; Hirano et al., 2012). The functional disruption of DMN in dopamine-deficient PD individuals has been reported in several previous studies (Nagano-Saito et al., 2008; van Eimeren

et al., 2009; Ibarretxe-Bilbao et al., 2011; Tessitore et al., 2012). Tessitore et al. (2012) reported that the functional disruption in inferior parietal lobule and medial temporal lobe of DMN occurs in cognitively unimpaired PD patients, and the DMN connectivity changes may predict a cognitive decline at later stages of the disease. An activation study revealed that PD showed the reversed pattern of task-related DMN deactivation in posterior cingulate and precuneus, as well as its deactivation level to a lesser degree than healthy subjects (van Eimeren et al., 2009). We observed abnormal functional reorganization of PCC connectivity in bilateral inferior parietal lobule, cingulate and precuneus of DMN in PDC in comparison to HC.

We observed increased functional connectivity of PCC in parahippocampal gyrus and decreased in middle cingulate in PDICD compared to HC. In comparison to PDC, the DMN changes were relatively spared in the middle cingulate, but aberrantly elevated in the precuneus and inferior parietal lobule in PDICD. This may imply that the impairment of DMN in PDICD result as a secondary pathological process following repetition of drug-related pathological behaviors. Consistently, similar changes of DMN connectivity have been found in several psychiatric disorders associated with substance abuse and other forms of addictive behaviors, which showed DMN connectivity enhanced in hippocampus and diminished in anterior cingulate (Ma et al., 2010; Ma et al., 2011).

The underlying individual vulnerability to the drug-induced aberrant behavioral features in PD can be accounted by specific risk factors such as sex, age at PD onset, personality traits and familial history of addictive disorders (Antonini & Cilia, 2009). The network reorganization in medicated PD with ICD could possibly emerge from some combination of the factors and the pathophysiology of the disorder in susceptible individuals. More

investigations to provide insights into the neurophysiological aspects of the behavioral disturbances and to discuss strategies for prevention and management in PD will be necessary. The present study has several limitations including a small sample size. Also, the study does not include drug-naive patients. Hence, it is limited to support the idea that emergence of ICD in PD and the functional remapping of the brain networks in PD with ICD are related to the dopaminergic medication effects. Furthermore, functional connectivity studies do not make any explicit notions regarding the causal relationships between the diseased conditions or medication effects and the functional connectivity alterations, therefore, the observations in this study do not allow any inferences of the causal interactions. Future studies with a larger sample size including drug-naive patients in order to consider the medications effects on the functional network changes in PD with ICD will be necessary.

CONCLUSION

The functional disconnections of striatum in many cortical areas result as a neurodegenerative process of dopaminergic mesocorticolimbic system in PD, however, the functional connectivity in parahippocampal gyrus encompassing hippocampus and amygdala was enhanced. The spatial reorganization of the functional striatal network involving the parahippocampal gyrus and insula may underlie the development of psychiatric disorders in PD. The plastic changes of the striatum in the thalamus may be also related to the drug-induced complication in vulnerable PD patients. Repetitive exposure to pathological behavioral stimuli may lead to the network changes within DMN, particularly in the precuneus, cingulate and inferior parietal lobule in PDICD.

REFERENCES

Aarsland D, Larsen JP, Lim NG, Janvin C, Karlsen K, Tandberg E & Cummings JL. Range of neuropsychiatric disturbances in patients with Parkinson's disease. J Neurol Neurosurg Psychiatry. 1999; 67: 492-6.

Antonini A, Cilia R. Behavioural adverse effects of dopaminergic treatments in Parkinson's disease: incidence, neurobiological basis, management and prevention. Drug Saf. 2009; 32(6): 475-88.

Baler RD, Volkow ND. Drug addiction: the neurology of disrupted self-control. Trends Mol Med. 2006; 12(12): 559-66.

Bechara A. Decision making, impulse control and loss of willpower to resist drugs: a neurocognitive perspective. Nat Neurosci. 2005; 8(11): 1458-63.

Biswal B, Yetkin FZ, Haughton VM, Hyde JS. Functional connectivity in the motor cortex of resting human brain using echo-planar MRI. Magn Reson Med. 1995; 34(4): 537-41.

Bonnet AM, Jutras MF, Czernecki V, Corvol JC, Vidailhet M. Nonmotor symptoms in Parkinson's disease in 2012: relevant clinical aspects. Parkinson's disease. 2012: doi:10.1155/2012/198316.

Broyd SJ, Demanuele C, Debener S, Helps SK, James CJ, Sonuga-Barke EJ. Default-mode brain dysfunction in mental disorders: a systematic review. Neurosci Biobehav Rev. 2009; 33(3): 279-96.

Cilia R, Cho SS, van Eimeren T, Marotta G, Siri C, Ko JH, Pellecchia G, Pezzoli G, Antonini A, Strafella AP. Pathological gambling in patients with Parkinson's disease is associated with fronto-striatal disconnection: a path

modeling analysis. Mov Disord. 2011; 26(2): 225-33.

Cilia R, Siri C, Marotta G, Isaias IU, De Gaspari D, Canesi M, Pezzoli G, Antonini A. Functional abnormalities underlying pathological gambling in Parkinson disease. Arch Neurol. 2008; 65(12): 1604-11.

Dagher A, Owen AM, Boecker H, Brooks DJ. The role of the striatum and hippocampus in planning: a PET activation study in Parkinson's disease. Brain. 2001; 124(Pt5): 1020-32.

Dang LC, Donde A, Madison C, O'Neil JP, Jagust WJ. Striatal dopamine influences the default mode network to affect shifting between object features. J Cogn Neurosci. 2012; 24(9): 1960-70.

Di Martino A, Scheres A, Margulies DS, Kelly AM, Uddin LQ, Shehzad Z, Biswal B, Walters JR, Castellanos FX, Milham MP. Functional connectivity of human striatum: a resting state FMRI study. Cereb Cortex. 2008; 18(12): 2735-47.

Dodd ML, Klos KJ, Bower JH, Geda YE, Josephs KA, Ahlskog JE. Pathological gambling caused by drugs used to treat Parkinson disease. Arch Neurol. 2005; 62(9): 1377-81.

Driver-Dunckley E, Samanta J, Stacy M. Pathological gambling associated with dopamine agonist therapy in Parkinson's disease. Neurology. 2003; 61(3): 422-3.

Fox MD, Greicius M. Clinical applications of resting state functional connectivity. Front Syst Neurosci. 2010; 4(19): 1-13. doi: 10.3389/fnsys.2010.00019.

Fox MD, Raichle ME. Spontaneous fluctuations in brain activity observed with functional magnetic resonance imaging. Nat Rev Neurosci. 2007; 8(9):

700-11.

Friston KJ. Functional and effective connectivity in neuroimage: a synthesis. Hum Brain Mapp. 1994; 2: 56-78.

Frucht S, Rogers JD, Greene PE, Gordon MF & Fahn S. Falling asleep at the wheel: motor vehicle mishaps in persons taking pramipexole and ropinirole. Neurology. 1999: 52(9): 1908-10.

Ghosh A, Rho Y, McIntosh AR, Kötter R, Jirsa VK. Noise during rest enables the exploration of the brain's dynamic repertoire. PloS Comput Biol. 2008; 4(10): e1000196. doi: 10.1371/journal.pcbi.1000196.

Goldstein RZ, Tomasi D, Rajaram S, Cottone LA, Zhang L, Maloney T, Telang F, Alia-Klein N, Volkow ND. Role of the anterior cingulate and medial orbitofrontal cortex in processing drug cues in cocaine addiction. Neuroscience. 2007; 144(4): 1153-9.

Greicius M. Resting-state functional connectivity in neuropsychiatric disorders. Curr Opin Neurol. 2008; 21(4): 424-30.

Hacker CD, Perlmutter JS, Criswell SR, Ances BM & Snyder AZ. Resting state functional connectivity of the striatum in Parkinson’s disease. Brain. 2012; 135: 3699-711.

Hacker CD, Perlmutter JS, Criswell SR, Ances BM, Snyder AZ Resting state functional connectivity of the striatum in Parkinson's disease. Brain. 2012; 135(Pt 12): 3699-711.

He BJ, Snyder AZ, Zempel JM, Smyth MD, Raichle ME. Electrophysiological correlates of the brain's intrinsic large-scale functional architecture. Proc Natl Acad Sci U S A. 2008; 105(41): 16039-44.

Helmich RC, Derikx LC, Bakker M, Scheeringa R, Bloem BR & Toni I.

Spatial remapping of cortico-striatal connectivity in Parkinson's disease. Cereb Cortex. 2010; 20: 1175-86.

Hirano S, Shinotoh H, Eidelberg D. Functional brain imaging of cognitive dysfunction in Parkinson's disease. J Neurol Neurosurg Psychiatry. 2012; 83(10): 963-9.

Ibarretxe-Bilbao N, Zarei M, Junque C, Marti MJ, Segura B, Vendrell P, Valldeoriola F, Bargallo N, Tolosa E. Dysfunctions of cerebral networks precede recognition memory deficits in early Parkinson's disease. Neuroimage. 2011; 57(2): 589-97.

Kelly C, de Zubicaray G, Di Martino A, Copland DA, Reiss PT, Klein DF, Castellanos FX, Milham MP, McMahon K. L-dopa modulates functional connectivity in striatal cognitive and motor networks: a double-blind placebo-controlled study. J Neurosci. 2009; 29(22): 7364-78.

Lee JS, Lee DS. Analysis of functional brain images using population-based probabilistic Atlas. Curr Med Imaging Rev 2005;1: 81–7.

Lee JY, Kim JM, Kim JW, Cho J, Lee WY, Kim HJ, Jeon BS. Association between the dose of dopaminergic medication and the behavioral disturbances in Parkinson disease. Parkinsonism Relat Disord. 2010; 16: 202–7.

Lee JY, Lee EK, Park SS, Lim JY, Kim HJ, Kim JS, Jeon BS. Association of DRD3 and GRIN2B with impulse control and related behaviors in Parkinson's disease. Mov Disord, 2009; 24: 1803–10.

Lee JY, Seo SH, Kim YK, Yoo HB, Kim YE, Song IC, Lee JS, Jeon BS. Extrastriatal dopaminergic changes in Parkinson's disease patients with impulse control disorders. J Neurol Neurosurg Psychiatry. 2014; 85(1): 23-30.

Ma N, Liu Y, Fu XM, Li N, Wang CX, Zhang H, Qian RB, Xu HS, Hu X,

Zhang DR. Abnormal brain default-mode network functional connectivity in drug addicts. PLoS One. 2011; 6(1): e16560. doi: 10.1371/journal.pone.0016560.

Ma N, Liu Y, Li N, Wang CX, Zhang H, Jiang XF, Xu HS, Fu XM, Hu X, Zhang DR. Addiction related alteration in resting-state brain connectivity. Neuroimage. 2010; 49(1): 738-44.

MacDonald PA, Monchi O. Differential effects of dopaminergic therapies on dorsal and ventral striatum in Parkinson's disease: implications for cognitive function. Parkinson's disease. 2011: doi:10.4061/2011/572743.

Molina JA, Sáinz-Artiga MJ, Fraile A, Jiménez-Jiménez FJ, Villanueva C, Ortí-Pareja M, Bermejo F. Pathologic gambling in Parkinson's disease: a behavioral manifestation of pharmacologic treatment? Mov Disord. 2000; 15(5): 869-72.

Moskovitz C, Moses H & Klawans HL. Levodopa-induced psychosis: a kindling phenomenon. Am J Psychiatry. 1978; 135(6): 669-75.

Nagano-Saito A, Leyton M, Monchi O, Goldberg YK, He Y, Dagher A. Dopamine depletion impairs frontostriatal functional connectivity during a set-shifting task. J Neurosci. 2008; 28(14): 3697-706.

Naqvi NH, Bechara A. The hidden island of addiction: the insula. Trends Neurosci. 2009; 32(1): 56-67.

Naqvi NH, Rudrauf D, Damasio H, Bechara A. Damage to the insula disrupts addiction to cigarette smoking. Science. 2007; 315(5811): 531-4.

Owen AM, Roberts AC, Hodges JR, Summers BA, Polkey CE, Robbins TW. Contrasting mechanisms of impaired attentional set-shifting in patients with frontal lobe damage or Parkinson's disease. Brain. 1993; 116 (Pt5): 1159-75.

Potenza MN, Steinberg MA, Skudlarski P, Fulbright RK, Lacadie CM, Wilber MK, Rounsaville BJ, Gore JC, Wexler BE. Gambling urges in pathological gambling: a functional magnetic resonance imaging study. Arch Gen Psychiatry. 2003; 60(8): 828-36.

Rakshi JS, Uema T, Ito K, Bailey DL, Morrish PK, Ashburner J, Dagher A, Jenkins IH, Friston KJ, Brooks DJ. Frontal, midbrain and striatal dopaminergic function in early and advanced Parkinson's disease A 3D [(18)F]dopa-PET study. Brain. 1999; 122(Pt9): 1637-50.

Ray N, Strafella AP. Dopamine, reward, and frontostriatal circuitry in impulse control disorders in Parkinson's disease: insights from functional imaging. Clin EEG Neurosci. 2010; 41(2): 87-93.

Reiff J, Jost WH. Drug-induced impulse control disorders in Parkinson's disease. J Neurol. 2011; 258 (Suppl 2): S323-7.

Rieck RW, Ansari MS, Whetsell WO Jr, Deutch AY, Kessler RM. Distribution of dopamine D2-like receptors in the human thalamus: autoradiographic and PET studies. Neuropsychopharmacology. 2004; 29(2): 362-72.

Rogers RD, Sahakian BJ, Hodges JR, Polkey CE, Kennard C, Robbins TW. Dissociating executive mechanisms of task control following frontal lobe damage and Parkinson's disease. Brain. 1998; 121(Pt5): 815-42.

Sutherland MT, McHugh MJ, Pariyadath V, Stein EA. Resting state functional connectivity in addiction: Lessons learned and a road ahead. Neuroimage. 2012; 62(4): 2281-95.

Tessitore A, Esposito F, Vitale C, Santangelo G, Amboni M, Russo A, Corbo D, Cirillo G, Barone P, Tedeschi G. Default-mode network connectivity in cognitively unimpaired patients with Parkinson disease. Neurology. 2012;

79(23): 2226-32.

Tomasi D, Volkow ND, Wang R, Telang F, Wang GL, Chang L, Ernst T, Fowler JS. Dopamine transporters in striatum correlate with deactivation in the default mode network during visuospatial attention. PLoS ONE. 2009; 4(6): e6102.

van Eimeren T, Monchi O, Ballanger B, Strafella AP. Dysfunction of the default mode network in Parkinson disease: a functional magnetic resonance imaging study. Arch Neurol. 2009; 66(7): 877-83.

van Eimeren T, Pellecchia G, Cilia R, Ballanger B, Steeves TD, Houle S, Miyasaki JM, Zurowski M, Lang AE, Strafella AP. Drug-induced deactivation of inhibitory networks predicts pathological gambling in PD. Neurology. 2010; 75(19): 1711-6.

Voon V & Fox SH. Medication-related impulse control and repetitive behaviors in Parkinson disease. Arch Neurol. 2007; 64(8): 1089-96.

Wang K, Liang M, Wang L, Tian L, Zhang X, Li K, Jiang T. Altered functional connectivity in early Alzheimer's disease: a resting-state fMRI study. Hum Brain Mapp. 2007; 28(10): 967-78.

Weintraub D, Siderowf AD, Potenza MN, Goveas J, Morales KH, Duda JE, Moberg PJ, Stern MB. Association of dopamine agonist use with impulse control disorders in Parkinson disease. Arch Neurol. 2006; 63(7): 969-73.

Zhang D, Raichle ME. Disease and the brain's dark energy. Nat Rev Neurol. 2010; 6(1): 15-28.

국문 초록

충동조절장애를 가진 파킨슨 병에서의 선조체 및 내정상태회로의 기능적 연결성 패턴의 변화

신 성 아

서울대학교 자연과학대학

WCU 뇌인지과학과 전공

충동 조절 장애 (Impulse control disorder, ICD)는 파킨슨 병 환자들에서 도파민성 약물 치료에 동반되어 나타난다. 파킨슨 병은 기저핵 (Basal ganglia)내에 도파민 신경이 감쇠하면서 나타나는 퇴행성 질환으로, 충동 조절 장애를 동반한 파킨슨 병 환자에서의 기저핵의 선조체 (Striatum)와 대뇌 피질 (Cerebral cortex) 및 피질하 영역 (Subcortical regions)간의 기능적 연결성 (Functional connectivity) 및 내정상태회로 (Default mode network, DMN) 연결성 패턴의 변화를 고찰하기 위하여, 본 연구에서는 휴지상태 기능자기공명영상 (Resting-state functional magnetic resonance imaging, rs-fMRI)을 실시하였다. 9명의

정상군 (Healthy controls, HC), 8명의 충동 조절 장애가 없는 파킨슨 병 환자군 (Parkinson's disease controls, PDC), 10명의 충동 조절 장애가 있는 파킨슨 병 환자군 (Parkinson's disease with ICD, PDICD)을 대상으로 선조체의 미상핵 (Head of caudate nucleus), 전측 피각 (Anterior putamen), 후측 피각 (Posterior putamen), 그리고 내정상태회로의 일부인 후측 대상 피질 (Posterior cingulate cortex)을 seed영역으로 잡아 voxel-wise 기능적 연결성 상관관계맵을 계산하여 그룹간의 비교를 하였다.

본 연구에서는 전체 파킨슨 병 환자군에서 퇴행성 과정으로 인하여 선조체 영역이 많은 대뇌 피질 영역과의 기능적 연결성이 떨어지는 반면, 해마방회 (Parahippocampal gyrus)에서의 연결성이 증가하는 것을 관찰하였다. 이는 파킨슨 병에서 주요 손상이 심한 도파민성 흑질선조체로 (Nigrostriatal pathway)에 비하여 비교적 보존된 도파민성 대뇌변연계 (Mesolimbic system)의 약물에 의한 가소성 변화에 인하여 증가 되는 것으로 보인다. 충동 조절 장애가 있는 환자군에서 없는 환자군에 비해 피각과 소뇌간의 기능적 연결성이 감퇴하였으나, 기저핵과 소뇌의 기능적 저하에 대한 보상 기전에 의함으로 예측되는 중심전회 (Precentral gyrus)와 중심후회 (Postcentral gyrus)의 연결성 증가를 관찰하였다. 또한, 충동 조절 장애가 있는 파킨슨 병 환자군에서, 충동 조절 및 반응 억제에 관련된 뇌 네트워크의 부분인 해마방회, 섬엽 (insula)에서 선조체와의 기능적 초연결성 (Hyperconnectivity)이 나타났다. 이와 같은 변화는 파킨슨 병에서의 뇌 네트워크의 기능 이상이 충동 조절 장애의 발병을

촉진하여 나타나거나, 장애에 의한 2차 변화로 발생하는 것으로 생각해 볼 수 있다. 본 연구 결과에 따르면 시상을 포함한 선조체 네트워크의 약물에 의한 기능 장애 역시 파킨슨 병에서 충동 조절 장애의 발생에 연관이 있음을 보인다.

정상군에 비하여 충동 조절 장애가 없는 파킨슨 병 환자군에서 아래마루소엽 (Inferior parietal lobule), 쐐기앞소엽 (Precuneus), 중간 대상회 (Middle cingulate)을 포함한 몇 몇의 영역에서 내정상태회로의 무결성 (Integrity)이 눈에 띄게 침체되는 것을 관찰하였다. 그에 반해서, 충동 조절 장애를 가진 파킨슨 병 환자군에서 해마 (Hippocampus)와 쐐기앞소엽에서 내정상태회로 연결성이 증가하였고, 중간 대상회에서는 감소하는 것을 보였다. 충동 조절 장애가 있는 환자군과 없는 환자군의 비교 결과, 장애가 있는 환자군에서 아래마루소엽, 대상회, 쐐기앞소엽에서 약물 유발성 행동 변화에 의해 발생된 것으로 보이는 기능적 증대를 관찰하였다.

주요어: *파킨슨 병, 충동 조절 장애, 기능적 연결성, 휴지상태 기능자기공명영상, 선조체, 내정상태회로*

학번: *2012-22520*